The Journal of Chemical Physics

Transferability of machine learning potentials: Protonated water neural network potential applied to the protonated water hexamer

Cite as: J. Chem. Phys. **154**, 051101 (2021); https://doi.org/10.1063/5.0035438
Submitted: 28 October 2020 • Accepted: 08 January 2021 • Published Online: 01 February 2021

Christoph Schran, Fabien Brieuc and Dominik Marx

The Journal of Chemical Physics COMMUNICATION scitation.org/journal/jcp

Transferability of machine learning potentials: Protonated water neural network potential applied to the protonated water hexamer

Cite as: J. Chem. Phys. 154, 051101 (2021); doi: 10.1063/5.0035438
Submitted: 28 October 2020 • Accepted: 8 January 2021 •
Published Online: 1 February 2021

Christoph Schran,[1,2,a)] Fabien Brieuc,[1] and Dominik Marx[1,b)]

AFFILIATIONS

[1] Lehrstuhl für Theoretische Chemie, Ruhr-Universität Bochum, 44780 Bochum, Germany
[2] Department of Physics and Astronomy, University College London, London WC1E 6BT, United Kingdom

[a)] **Author to whom correspondence should be addressed:** christoph.schran@rub.de. **Present address:** Department of Chemistry, University of Cambridge, Lensfield Road, Cambridge CB2 1EW, United Kingdom.
[b)] **Electronic mail:** dominik.marx@rub.de

ABSTRACT

A previously published neural network potential for the description of protonated water clusters up to the protonated water tetramer, $H^+(H_2O)_4$, at an essentially converged coupled cluster accuracy [C. Schran, J. Behler, and D. Marx, J. Chem. Theory Comput. **16**, 88 (2020)] is applied to the protonated water hexamer, $H^+(H_2O)_6$—a system that the neural network has never seen before. Although being in the extrapolation regime, it is shown that the potential not only allows for quantum simulations from ultra-low temperatures ~1 K up to 300 K but is also able to describe the new system very accurately compared to explicit coupled cluster calculations. This transferability of the model is rationalized by the similarity of the atomic environments encountered for the larger cluster compared to the environments in the training set of the model. Compared to the interpolation regime, the quality of the model is reduced by roughly one order of magnitude, but most of the difference to the coupled cluster reference comes from global shifts of the potential energy surface, while local energy fluctuations are well recovered. These results suggest that the application of neural network potentials in extrapolation regimes can provide useful results and might be more general than usually thought.

I. INTRODUCTION

In recent years, machine learning has become a compelling tool for the representation of potential energy surfaces.[1–6] The first family of such machine learning potentials based on artificial neural networks that scale to arbitrary system sizes were high-dimensional neural network potentials[7,8] (NNPs). Since then, many distinctly different approaches either also based on artificial neural networks[9–15] or on kernel methods[16–21] have been introduced over the years, while recent development following the principles of deep learning has allowed one to incorporate parts of the description of the chemical environments in the architecture of the model.[22,23] While there is usually agreement in the community that these models can only be used in order to interpolate between a meaningful set of training points, there have been recent examples that show a broader transferability of such machine learning approaches than those previously assumed. This includes the application of NNPs[7,8] for alkanes to larger chains[24] and for liquid water to various ice phases[25] as well as a Gaussian approximation potential[16] for carbon to random structure searches[26] that explored quite different configurations than the diverse carbon phases used to train the model.

In this communication, we show that such a generalization capability can also be obtained for protonated water clusters of larger size than the clusters used in the training set of the machine learning model. For that purpose, we use our previously published NNP (exactly as reported in the supplementary material of Ref. 27) for the description of protonated water clusters, which has been developed in an automated and adaptive workflow. It has been trained on essentially converged coupled cluster reference data for protonated water clusters up to $H^+(H_2O)_4$—including also the water

monomer itself. This implies that the very same model is able to describe the potential energy surface of all differently sized clusters $H^+(H_2O)_n$ (here from $n = 1$ up to 4) on equal footing by virtue of including all of them explicitly and simultaneously in the training. In contrast, conventional many-body expansions, which have also been successfully applied to protonated water clusters,[28] expand the potential energy as a sum of many-body *corrections* to the previous terms.

Here, we apply our model to path integral molecular dynamics (PIMD) quantum simulations of the protonated water hexamer, $H^+(H_2O)_6$, in its extended Zundel conformation (i.e., the hydrated protonated water dimer), a system that was not included in training the NNP. The structures generated by these stable quantum simulations are afterward validated with respect to single-point coupled cluster calculations of the same quality as those used to generate the NNP up to $n = 4$ only. We show that this particular model is able to provide meaningful and accurate predictions in this extrapolation regime. These promising results are rationalized by the similarity of the atomic environments encountered in this extrapolation regime to the ones obtained for the smaller protonated water clusters present in the training set of the model.

II. RESULTS AND DISCUSSION

In order to test the application of the previously published NNP for the description of protonated water clusters beyond what was considered in the original development,[27] we ran path integral simulations at various temperatures starting from the optimized minimum energy structure of the extended Zundel cation. The computational details of these simulation are described in the Appendix. All tested quantum simulations from close to the ground state at 1.67 K up to 100 K were stable—although all being evidently in the extrapolation regime of the NNP. The model was indeed exclusively extrapolating since for each and every configuration encountered during the simulations, the associated values of the atom-centered symmetry functions,[30] used here as descriptors of the atomic environments, were outside the range of values present during training. In particular, we mainly observe the extrapolation of the two broadest radial symmetry functions: one centered around oxygen atoms and the other one centered around hydrogen atoms, both of which involve distant oxygen atoms in their pairs. This indicates that exclusively unknown configurations were encountered in all steps of these simulations. While simulations up to 100 K sampled only the extended Zundel isomer, $H_5O_2^+(H_2O)_4$, we applied the model also at temperatures of 200 K, 250 K, and 300 K, which resulted in occasional rearrangements of the cluster to other known minima. Out of the 12 simulations at higher temperatures, two runs rearranged into strained four-membered ring structures for which the NNP provided unphysical predictions after about a 200 ps simulation time, a phenomenon we analyze in more detail toward the end of this communication. This mostly stable application of the NNP in an extrapolation regime is a first promising indication that the potential could be applied beyond the originally considered cluster sizes.

In Fig. 1, we show the probability distribution functions of three main structural properties of the hydrogen bond[31] from the simulation of $(H_5O_2^+)(H_2O)_4$ at 1.67 K and compare them to the respective

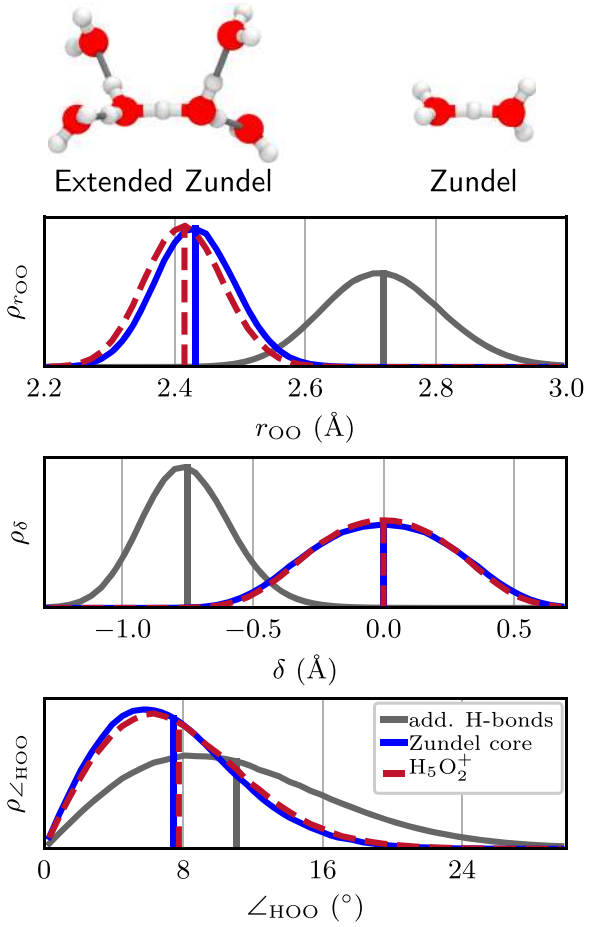

FIG. 1. Normalized probability distributions of the heavy atom donor–acceptor distance r_{OO} (top), the proton-sharing coordinate δ (middle) defined as $\delta = r_{OH} - r_{H\cdots O}$, and the hydrogen bond angle $\angle_{HOO}$ (bottom) from PIMD simulations at 1.67 K for the central ultra-strong hydrogen bond (blue) and the additional four hydrogen bonds to the dangling water molecules (gray) in the extended Zundel cation, $(H_5O_2^+)(H_2O)_4$, as well as for the smaller bare Zundel cluster, $H_5O_2^+$, (red) for comparison. The average of the distributions is marked with vertical lines using the same color code. Only hydrogen bonded configurations are considered in this analysis based on a standard hydrogen bond criterion.[29] The optimized minimum energy structures of the two considered systems are displayed on top of the figure.

distributions of the much smaller bare Zundel cation, $H_5O_2^+$. As shown therein, the model provides the expected bimodal distributions of the donor–acceptor distance r_{OO} and the proton-sharing coordinate δ for the extended Zundel cation, caused by the two distinctly different types of hydrogen bonds in the system: the central ultra-strong hydrogen bond (shown in blue) and the four additional hydrogen bonds to the dangling water molecules (shown in gray). In comparison, the bare Zundel complex has qualitatively similar distributions in the case of the central hydrogen bond but features a distinct shift toward shorter donor–acceptor distances as well as a slightly more localized proton-sharing coordinate. Finally, the distribution of the HOO angle for the central ultra-strong hydrogen bond in the extended Zundel cation is again close to the one in the bare

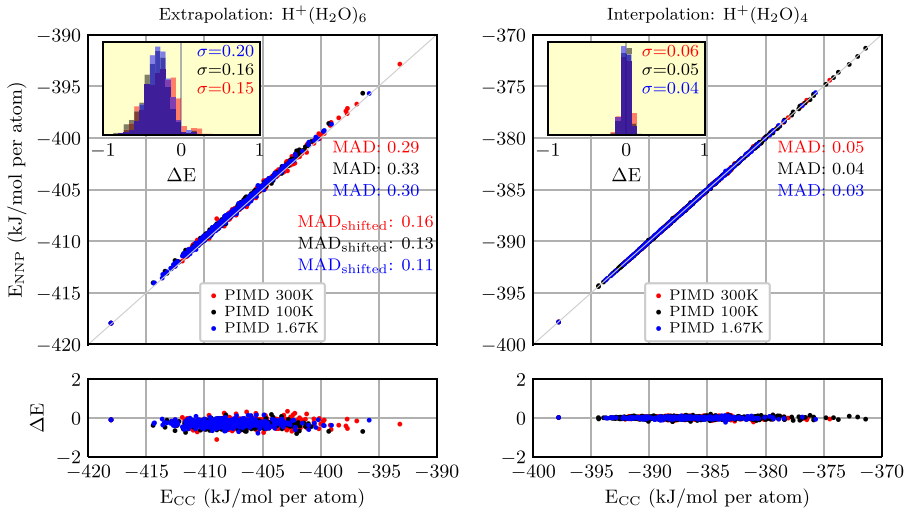

FIG. 2. Correlation of the energy per atom from explicit CCSD(T*)-F12a/aug-cc-pVTZ calculations (CC) and the NNP predictions for 300 randomly selected configurations of the protonated water hexamer (left panels) and the protonated water tetramer in its Eigen-conformation (right panels) at 1.67 K (blue), 100 K (black), and 300 K (red), respectively. The mean absolute differences (MAD) for all temperatures are reported in their respective color. In the upper left panel, we also include the shifted MAD values (see text), for which the systematic bias (as quantified in the upper left inset) is removed from the NNP prediction by shifting the energies by the MAD at the respective temperature (but without showing the underlying shifted data themselves). The lower panels show the energy differences between CC reference and NNP prediction over the whole range of reference energies, while the inset in the upper panels shows the histograms of the energy differences including the corresponding standard deviations σ in the respective color.

Zundel complex, while the four weaker hydrogen bonds to the dangling water molecules feature the expected broader distribution that is shifted to larger angles. These results are in substantial agreement with the previous studies on the extended Zundel cation[32–37] regarding the symmetric nature of the central ultra-strong hydrogen bond and its close match with that in the smaller bare Zundel cation. This highlights the physically meaningful nature of the quantum structures generated with our model operating here in the extrapolation mode, even close to the quantum ground state at 1.67 K.

In a next step, the quality of the NNP prediction during the simulations is validated by explicitly evaluating the coupled cluster reference method [namely, CCSD(T*)-F12a/aug-cc-pVTZ; see the Appendix for details] for 300 randomly selected configurations at 1.67 K, 100 K, and 300 K. We note that due to the system size, such coupled cluster calculations are increasingly demanding in view of their steep scaling not only in terms of computation time but also when it comes to memory resources. This growth is such that it would have been challenging to explicitly include the protonated

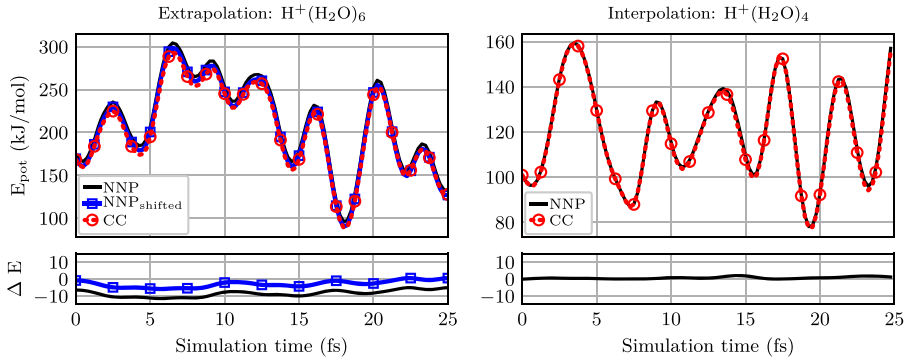

FIG. 3. Potential energy along one replica of quantum PIMD trajectories at 1.67 K of the extended Zundel cation (left) and the protonated water tetramer in the Eigen-conformation (right) using the original and shifted (see the text) neural network potentials (NNP, $NNP_{shifted}$ only in the left panel). The CCSD(T*)-F12a/aug-cc-pVTZ reference (CC) is obtained by recomputing the energies for each configuration along the NNP trajectories and is shown as red dotted lines (with only a few circles added since the CC energies mostly superimpose the NNP data). These energies are reported relative to the respective equilibrium structure. The bottom panels highlight the respective energy differences in the NNP predictions to the CC reference method.

water hexamer when training the NNP in the first place. The resulting correlation of the NNP prediction and the actual coupled cluster reference for $H^+(H_2O)_6$ is shown in the left panels of Fig. 2. In the same figure, we include in the right panels the equivalent test for the largest cluster considered during the development of that NNP, namely, the protonated water tetramer, $H^+(H_2O)_4$, in its Eigen structure (corresponding to the hydrated hydronium cation/protonated water monomer H_3O^+). Note that the same energy scales are used for all axes to allow for one-to-one comparisons. Overall, a high correlation between reference and NNP is obtained, which is especially remarkable for a NNP that operates exclusively in the extrapolation regime as is the case for the protonated water hexamer (left panels). The application of NNPs in interpolation regimes, as demonstrated here for $H^+(H_2O)_4$ (right panels), is evidently yielding better results, but the quality of the NNP for the larger and thus fully extrapolating system is only reduced by about one order of magnitude and—most importantly—does not feature strong outliers for all 300 configurations considered in this cross-check. In addition, it can be seen that the prediction of the NNP in the extrapolation regime is affected by a systematic bias as evident from the shift of the histogram of the energy differences with respect to zero shown in the inset of the upper left panel. If this bias is removed from the prediction of the NNP by uniformly shifting all energies by the respective mean absolute difference (here 0.30 kJ/mol, 0.33 kJ/mol, and 0.29 kJ/mol per atom at 300 K, 100 K, and 1.67 K, respectively), the precision of the prediction is improved roughly by a factor of three at no additional cost. We note in passing that we observe essentially the same quality for the low temperature simulations that sample exclusively the extended Zundel conformer, as for the configurations at 300 K, although rearrangements to other known minima occur under these conditions.

To further validate the application of the NNP for the extended Zundel cation when used in realistic simulations, we additionally re-evaluated a short segment of the trajectory associated with one replica, or bead, of the quantum path integral molecular dynamics simulations at 1.67 K with the coupled cluster reference method. The resulting potential energy profile along these 25 fs of the simulation is shown in the left panel of Fig. 3. We also carried out the same analysis for the largest cluster explicitly considered in the construction of the NNP, the protonated water tetramer, in the right panel to allow for one-to-one comparison to the interpolation regime. As before, the NNP yields surprisingly good results for the extended Zundel cation, although working exclusively in its extrapolation mode. The NNP is found to be able to recover the overall energy profile along the short segment of the trajectory and correctly reproduces the energy fluctuations (black line). As already seen for the randomly selected structures, the NNP is affected by an overall bias that shifts the prediction to slightly larger energies. However, if we use the mean absolute difference of the 300 random structures from the simulation at 1.67 K to shift the energy prediction according to the NNP, the coupled cluster reference energy profile is recovered perfectly by the $NNP_{shifted}$ on the physically relevant scale as set by the potential energy fluctuations (blue line with squares). As known from the originally published benchmarking of the NNP,[27] the Eigen cation does not suffer from such a bias since it has been used explicitly to train that NNP, as shown in the right panel of Fig. 3. Overall, this analysis reveals that the fully extrapolating NNP is able to almost perfectly recover the correct energy fluctuations of the extended Zundel cation even in the deep quantum regime at 1.67 K close to the ground state after correcting for the global energy shift. Even without any such shift of the energies, the NNP performs unexpectedly well in such an extrapolation regime, which suggests that there can be great potential in exploiting extrapolation capabilities for building more complex machine learning potentials.

Let us finally provide some insight into the unexpected transferability of the model to the protonated water hexamer. In order to check whether the predictive power of our model is the sole result of the similarity to the protonated water tetramer, we have trained a separate NNP only to the tetramer configurations present in the training set. This model could not be successfully applied in PIMD simulations as rearrangements into unphysical configurations are

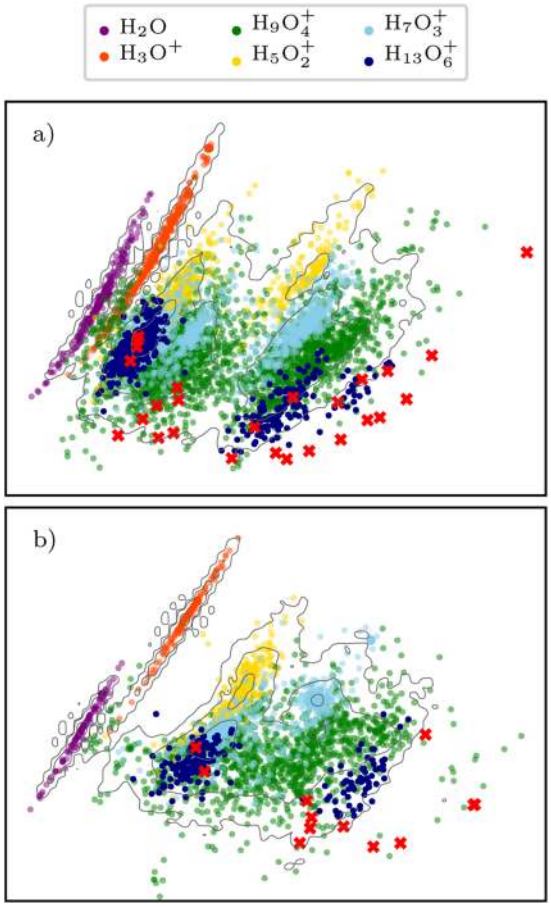

FIG. 4. Two dimensional projection based on the principle component analysis of the hydrogen (a) and oxygen (b) atomic environments as encoded by the atom centered symmetry functions of the training set of the NNP model. The differently sized clusters for a subset of the atomic environments in the training set are marked by different colors, while the contour lines show the probability density of the PCA projection for all atomic environments in the training set in equidistant steps on a logarithmic scale. The same projection, shown in dark blue, is also applied to the configurations of the protonated water hexamer as generated by PIMD simulations at various temperatures. Red crosses mark the atomic environments of two configurations of the protonated water hexamer, which feature unphysical predictions of the NNP model.

observed at all temperatures after some short initial period. We thus conclude that the smaller clusters grant additional robustness to the model and contribute to its transferability.

To further understand this behavior, we have analyzed the similarity of the atomic environments encountered in the extrapolation regime, as encoded by the atom centered symmetry functions, to the environments in the training set of the model. For that purpose, we performed a principle component analysis (PCA), separately for the oxygen and hydrogen environments, and projected the descriptors onto the two most relevant components. These two components together account for 72% and 82% of the variance in the full dimensional feature space of oxygen and hydrogen environments, respectively. Subsequently, the same projection is applied to the configurations of the protonated water hexamer, as depicted in Fig. 4. As shown by the dark blue points in this figure, the configurations of the protonated water hexamer remain within the boundaries of the training set for the most relevant components of the descriptor space, although we have observed extrapolation for a subset of the descriptors. This observation is in line with other recent studies that have reported on the generalization capabilities in machine learning models for various systems.[24–26]

In addition, we have also included the projection of the atomic environments in the two higher temperature conformers that feature strained four-membered rings and were observed to lead to unphysical predictions of the model (see the red crosses in Fig. 4). Clearly, the main components of these atomic environments leave the region spanned by the training set, which thus can be associated with the missing predictive power of the model. This points toward the limitations of the application of machine learning models in extrapolation regimes, as sufficient similarity to the training set is required to provide meaningful results. We note that these limitations can, in principle, be overcome by continuing the automated fitting process of the model and explicitly targeting the larger cluster by selecting the most representative configurations from our exhaustive simulations.

III. CONCLUSION AND OUTLOOK

In summary, our previously published neural network potential, trained for simulations up to the protonated water tetramer, performs unexpectedly well for the extended Zundel cation, a conformer of the protonated water hexamer. This is notable since these simulations are carried out entirely in the extrapolation regime, which means that only unknown configurations are encountered in each and every simulation step. This NNP does not only allow one to run stable path integral quantum simulations but also recovers correctly the quantum-thermal energy fluctuations in direct comparison to the coupled cluster reference data of the extended Zundel complex. Yet, the NNP suffers from a slight global shift of the potential energy, which, however, does not influence the relative fluctuations. Moreover, we show how this shift can be systematically corrected *a posteriori* based on rather few additional reference calculations of the extended complex.

These promising results are explained by the similarity of the atomic environments encountered in the present application with the environments of the smaller clusters that composed the training set of the model, which accurately treats a class of molecular complexes consisting of three up to 13 constituting atoms. Since the training set of the neural network potential is composed of clusters from the hydronium cation up to the protonated water tetramer and does include the water monomer as well, sufficient local environments are considered in its construction to yield these reassuring results.

Still, we would like to stress that these promising results should not be taken for granted and using machine learning models beyond their considered scope of application during their construction and parameterization requires great care and sufficient validation. Evidently, in most cases that are too far away from the chemical space spanned by the training set, machine learning models will provide unphysical results. We observed this in the present case at higher temperatures, where significant topological rearrangements can occur that generate distinctly different atomic environments in the protonated water clusters compared to those covered by our training set. At the same time, our results reveal that there can be cases where carefully constructed machine learning models are applicable much beyond interpolation regimes. This could be a promising route to the development of more complex machine learning models. Thus, we hope that our short report will stimulate methodological work to explore systematically and fundamentally the power of machine learning models to safely conquer unknown territory.

ACKNOWLEDGMENTS

We are thankful to Harald Forbert, Ondrej Marsalek, and Venkat Kapil for insightful discussions. This work was funded by the *Deutsche Forschungsgemeinschaft* (DFG, German Research Foundation) under Germany's Excellence Strategy (Grant No. EXC 2033-390677874-RESOLV). C.S. acknowledges partial financial support from the *Alexander von Humboldt-Stiftung*. The computational resources were provided by HPC@ZEMOS, HPC-RESOLV, and BoViLab@RUB.

APPENDIX: COMPUTATIONAL DETAILS

Path integral molecular dynamics simulations of the extended Zundel cation down to 1.67 K have been performed with the CP2k program package.[38,39] The potential energy surface was described using a recently developed and published NNP fitted to coupled cluster reference calculations.[27] This NNP describes all protonated water clusters, from the protonated water monomer (hydronium cation) up to the protonated water tetramer considered in the development, on equal footing and, in particular, also explicitly includes the water monomer. It has been shown to not only match the reference coupled cluster theory with very high precision but also able to accurately describe proton transfer in the considered clusters.[31] We apply this NNP[27] in the present study to the larger protonated water hexamer in its extended Zundel structures, which is thus entirely in the extrapolation regime of the model.

The extended Zundel cation was simulated at temperatures of 300 K, 250 K, 200 K, 100 K, 20 K, 10 K, and 1.67 K, including the quantum nature of the nuclei using the path integral quantum thermal bath (PIQTB) thermostat,[40] which has been recently extended to and validated at ultra-low temperatures.[41] In order to reach convergence, the path integral was discretized using P = 6, 8, 12, 16, 64, 128, and 256 replica at

T = 300 K, 250 K, 200 K, 100 K, 20 K, 10 K, and 1.67 K, respectively. The convergence of these path integral discretizations was chosen according to previous explicit benchmarking results[41] for the prototypical hydrogen bond in the bare Zundel cation. For comparison, we also performed simulations using exactly the same settings for the Eigen and bare Zundel clusters, which were explicitly considered in the construction of the model.[27] All reported simulations were propagated in four independent runs for, in total, 1 ns using a formal molecular dynamics time step of 0.25 fs, while 10 ps at the beginning of each simulation were discarded as equilibration.

Explicit validations of the predictive power of the NNP, which is used here exclusively in its extrapolation regime, was achieved by reevaluating the energies of many configurations of the extended Zundel complex with the same coupled cluster method as used for the development of that NNP. These calculations of the coupled cluster singles, doubles, and perturbative triples [CCSD(T)] reference energies were performed with the Molpro program package[42] by employing the explicitly correlated F12a method[43,44] to correct for the basis set incompleteness error. As suggested,[44] we additionally employed the size-consistent scaling of the perturbative triples, (T*), together with the aug-cc-pVTZ basis set.[45,46] This so-called CCSD(T*)-F12a/aug-cc-pVTZ electronic structure setup has been shown to provide energies very close to the complete basis set (CBS) limit.[44]

DATA AVAILABILITY

The data that support the findings of this study are available within the article.

REFERENCES

[1] J. Behler, J. Chem. Phys. **145**, 170901 (2016).
[2] A. P. Bartók, S. De, C. Poelking, N. Bernstein, J. R. Kermode, G. Csányi, and M. Ceriotti, Sci. Adv. **3**, e1701816 (2017).
[3] K. T. Butler, D. W. Davies, H. Cartwright, O. Isayev, and A. Walsh, Nature **559**, 547 (2018).
[4] V. L. Deringer, M. A. Caro, and G. Csányi, Adv. Mater. **31**, 1902765 (2019).
[5] T. Mueller, A. Hernandez, and C. Wang, J. Chem. Phys. **152**, 050902 (2020).
[6] S. Manzhos and T. Carrington "Neural network potential energy surfaces for small molecules and reactions," Chem. Rev. (published online).
[7] J. Behler and M. Parrinello, Phys. Rev. Lett. **98**, 146401 (2007).
[8] J. Behler, Angew. Chem., Int. Ed. **56**, 12828 (2017).
[9] S. A. Ghasemi, A. Hofstetter, S. Saha, and S. Goedecker, Phys. Rev. B **92**, 045131 (2015).
[10] A. Khorshidi and A. A. Peterson, Comput. Phys. Commun. **207**, 310 (2016).
[11] N. Artrith, A. Urban, and G. Ceder, Phys. Rev. B **96**, 014112 (2017).
[12] J. S. Smith, O. Isayev, and A. E. Roitberg, Chem. Sci. **8**, 3192 (2017).
[13] M. Gastegger, J. Behler, and P. Marquetand, Chem. Sci. **8**, 6924 (2017).
[14] O. T. Unke and M. Meuwly, J. Chem. Theory Comput. **15**, 3678 (2019).
[15] Y. Shao, M. Hellström, P. D. Mitev, L. Knijff, and C. Zhang, J. Chem. Inf. Model. **60**, 1184 (2020).
[16] A. P. Bartók, M. C. Payne, R. Kondor, and G. Csányi, Phys. Rev. Lett. **104**, 136403 (2010).
[17] M. Rupp, A. Tkatchenko, K. R. Müller, and O. A. Von Lilienfeld, Phys. Rev. Lett. **108**, 058301 (2012).
[18] A. P. Thompson, L. P. Swiler, C. R. Trott, S. M. Foiles, and G. J. Tucker, J. Comput. Phys. **285**, 316 (2015).
[19] A. V. Shapeev, Multiscale Model. Simul. **14**, 1153 (2015).
[20] Z. Li, J. R. Kermode, and A. De Vita, Phys. Rev. Lett. **114**, 096405 (2015).
[21] S. Chmiela, A. Tkatchenko, H. E. Sauceda, I. Poltavsky, K. T. Schütt, and K.-R. Müller, Sci. Adv. **3**, e1603015 (2017).
[22] K. T. Schütt, F. Arbabzadah, S. Chmiela, K. R. Müller, and A. Tkatchenko, Nat. Commun. **8**, 13890 (2017).
[23] L. Zhang, J. Han, H. Wang, R. Car, and E. Weinan, Phys. Rev. Lett. **120**, 143001 (2018).
[24] M. Gastegger, C. Kauffmann, J. Behler, and P. Marquetand, J. Chem. Phys. **144**, 194110 (2016).
[25] B. Monserrat, J. G. Brandenburg, E. A. Engel, and B. Cheng, Nat. Commun. **11**, 5757 (2020).
[26] P. Rowe, V. L. Deringer, P. Gasparotto, G. Csányi, and A. Michaelides, J. Chem. Phys. **153**, 034702 (2020).
[27] C. Schran, J. Behler, and D. Marx, J. Chem. Theory Comput. **16**, 88 (2020).
[28] P. Pinski and G. Csányi, J. Chem. Theory Comput. **10**, 68 (2014).
[29] A. Luzar and D. Chandler, Phys. Rev. Lett. **76**, 928 (1996).
[30] J. Behler, J. Chem. Phys. **134**, 074106 (2011).
[31] C. Schran and D. Marx, Phys. Chem. Chem. Phys. **21**, 24967 (2019).
[32] J.-C. Jiang, Y.-S. Wang, H.-C. Chang, S. H. Lin, Y. T. Lee, G. Niedner-Schatteburg, and H.-C. Chang, J. Am. Chem. Soc. **122**, 1398 (2000).
[33] R. A. Christie and K. D. Jordan, J. Phys. Chem. B **106**, 8376 (2002).
[34] Q. C. Nguyen, Y.-S. Ong, and J.-L. Kuo, J. Chem. Theory Comput. **5**, 2629 (2009).
[35] N. Heine, M. R. Fagiani, M. Rossi, T. Wende, G. Berden, V. Blum, and K. R. Asmis, J. Am. Chem. Soc. **135**, 8266 (2013).
[36] F. Mouhat, "Fully quantum dynamics of protonated water clusters," Ph.D. thesis, Sorbonne Université, 2018.
[37] J. P. Heindel, Q. Yu, J. M. Bowman, and S. S. Xantheas, J. Chem. Theory Comput. **14**, 4553 (2018).
[38] CP2K, freely available at the URL: https://www.cp2k.org, released under GPL license, 2020.
[39] J. Hutter, M. Iannuzzi, F. Schiffmann, and J. Vandevondele, Wiley Interdiscip. Rev.: Comput. Mol. Sci. **4**, 15 (2014).
[40] F. Brieuc, H. Dammak, and M. Hayoun, J. Chem. Theory Comput. **12**, 1351 (2016).
[41] C. Schran, F. Brieuc, and D. Marx, J. Chem. Theory Comput. **14**, 5068 (2018).
[42] H.-J. Werner, P. J. Knowles, G. Knizia, F. R. Manby, M. Schütz, P. Celani, W. Györffy, D. Kats, T. Korona, R. Lindh, A. Mitrushenkov, G. Rauhut, K. R. Shamasundar, T. B. Adler, R. D. Amos, S. J. Bennie, A. Bernhardsson, A. Berning, D. L. Cooper, M. J. O. Deegan, A. J. Dobbyn, F. Eckert, E. Goll, C. Hampel, A. Hesselmann, G. Hetzer, T. Hrenar, G. Jansen, C. Köppl, S. J. R. Lee, Y. Liu, A. W. Lloyd, Q. Ma, R. A. Mata, A. J. May, S. J. McNicholas, W. Meyer, T. F. Miller III, M. E. Mura, A. Nicklass, D. P. O'Neill, P. Palmieri, D. Peng, K. Pflüger, R. Pitzer, M. Reiher, T. Shiozaki, H. Stoll, A. J. Stone, R. Tarroni, T. Thorsteinsson, M. Wang, and M. Welborn, MOLPRO, version 2012.1, a package of *ab initio* programs.
[43] T. B. Adler, G. Knizia, and H.-J. Werner, J. Chem. Phys. **127**, 221106 (2007).
[44] G. Knizia, T. B. Adler, and H.-J. Werner, J. Chem. Phys. **130**, 054104 (2009).
[45] R. A. Kendall, T. H. Dunning, and R. J. Harrison, J. Chem. Phys. **96**, 6796 (1992).
[46] D. E. Woon and T. H. Dunning, Jr., J. Chem. Phys. **100**, 2975 (1994).